Acta Crystallographica Section B
Structural Science
ISSN 0108-7681

Supramolecular structures of 1-phenylethylammonium tartrates

David E. Turkington,[a] Elizabeth J. MacLean,[b] Alan J. Lough,[c] George Ferguson[a,d] and Christopher Glidewell[a]*

[a]School of Chemistry, University of St Andrews, St Andrews, Fife KY16 9ST, Scotland, [b]CCLRC Daresbury Laboratory, Daresbury, Warrington WA4 4AD, England, [c]Lash Miller Chemical Laboratories, University of Toronto, Toronto, Ontario, Canada M5S 3H6, and [d]Department of Chemistry, University of Guelph, Guelph, Ontario, Canada N1G 2W1

Correspondence e-mail: cg@st-andrews.ac.uk

Received 5 October 2004
Accepted 15 November 2004

The structures of six 1-phenylethylammonium tartrates have been determined and in each of them a distinctive hydrogen-bonded anion substructure can be identified. (*S*)-1-Phenylethylammonium (*R*,*R*)-hydrogen tartrate [(I), $P2_1$, $Z' = 1$] contains anion sheets built from a single type of $R_4^4(22)$ ring with cations pendent, *via* three N—H···O hydrogen bonds, from just one face of the sheet. (*S*)-1-Phenylethylammonium *rac*-hydrogen tartrate [(II), $P2_1$, $Z' = 2$] and its enantiomorph (*R*)-1-phenylethylammonium *rac*-hydrogen tartrate [(III), $P2_1$, $Z' = 2$] contain anion sheets built from four types of ring, $R_2^2(10)$, $R_2^2(12)$, $R_2^4(14)$ and $R_4^4(20)$, and there are cations pendent from both faces of the sheet. The anion substructure in bis[(*S*)-1-phenylethylammonium] (*R*,*R*)-tartrate [(IV), $P2_1$, $Z' = 1$] consists of simple $C(5)$ chains, which are linked into sheets by the cations, while in bis(*rac*-1-phenylethylammonium) (*R*,*R*)-tartrate [(V), $P2_1$, $Z' = 2$] there are anion sheets containing two distinct types of $R_4^4(22)$ ring, with equal numbers of (*R*) and (*S*) cations pendent from each face of the anion sheet. Bis[(*R*)-1-phenylethylammonium] *rac*-tartrate methanol hemisolvate [(VI), $P1$, $Z' = 4$, with 14 independent components in the asymmetric unit] contains anion sheets built from two types of $R_2^2(12)$ ring and two types of $R_6^6(32)$ ring; half of the cations and half of the methanol molecules are pendent from each face of the sheet.

1. Introduction

We have recently reported the supramolecular structures of the tartrate salts formed by a range of simple achiral diamines (Farrell *et al.*, 2002*a*) and one of the aims of that study was the comparison of cognate pairs of salts formed by the same amine, on the one hand with racemic tartaric acid and on the other with enantiopure (2*R*,3*R*)-tartaric acid. In those cases where the racemic and enantiopure acids formed pairs of salts with a common stoichiometry, the overall supramolecular structures of the two salts were very similar, despite their generally different space groups. Moreover, the salts formed by the (2*R*,3*R*) acid closely mimic centrosymmetry in a number of cases, a phenomenon also noted in the analogous salts formed by (*S*)-malic acid with a comparable range of achiral diamines (Farrell *et al.*, 2002*b*). Another feature of interest in the tartrate structures was the very wide range of anion substructures observed, including a variety of chains of fused rings and a variety of sheet substructures, as well as three-dimensional frameworks of anions encapsulating large voids which enclose the cations.

In view of this variety of anion substructures, but more particularly in view of the common mimicry of centrosymmetry, we have now extended this study to encompass systems in which the amine component is also chiral and for this

purpose we have selected 1-phenylethylamine, $PhCH(CH_3)NH_2$, which is readily available in both enantiopure forms, (*R*) and (*S*), as well as in the racemic form. Using the various stereochemical forms of this amine in combination with the various forms of tartaric acid, we have now prepared a range of 1:1 and 2:1 salts (I)–(VI), whose supramolecular structures we discuss here. The structure of (I) has previously been determined using ambient-temperature data (Molins *et al.*, 1989), but no analysis or discussion of the supramolecular aggregation was reported.

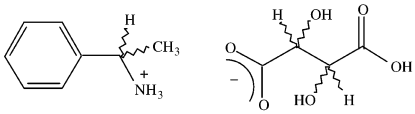

(I) (S)-cation (R,R)-anion
(II) (S)-cation rac-anion
(III) (R)-cation rac-anion

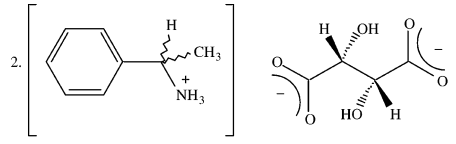

(IV) (S)-cation (R,R)-anion
(V) rac-cation (R,R)-anion

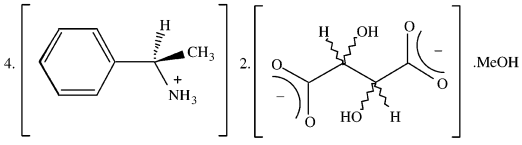

(VI) (R)-cation rac-anion

2. Experimental

2.1. Synthesis

Samples of racemic 1-phenylethylamine and enantiopure (*R*)- and (*S*)-1-phenylethylamine, and of racemic tartaric acid and enantiopure (*R*,*R*)-tartaric acid were purchased from Aldrich, and all were used as received. For the preparation of the phenylethylammonium tartrate salts, stoichiometric quantities of the appropriate amine and acid were separately dissolved in methanol. These solutions were then mixed and the mixtures were set aside to crystallize, providing analytically pure samples within a few days. Analyses: found for (I): C 53.1, H 6.7, N 5.1%; for (II): C 53.4, H 6.4, N 5.1%; for (III): C 52.7, H 6.4, N 5.0%: $C_{12}H_{17}NO_6$ requires C 53.1, H 6.3, N 5.2%: found for (IV): C 60.8, H 7.1, N 6.9%; for (V): C 60.3, H 7.2, N 7.0%; $C_{20}H_{28}N_2O_6$ requires C 61.2, H 7.2, N 7.1%: for (VI): C 60.1, H 7.4, N 6.8; $C_{41}H_{60}N_4O_{13}$ requires C 60.3, H 7.4, N 6.9%. For all except (V), satisfactory crystals suitable for single-crystal X-ray diffraction were selected directly from the prepared samples. For (V) the crystals were consistently of poor quality, despite a number of preparations under different conditions, and no useful data were obtained using a conventional laboratory radiation source; however, by use of synchrotron radiation a satisfactory dataset was obtained.

2.2. Data collection, structure solution and refinement

Diffraction data for (I)–(VI) were collected at 150 (1) K using Nonius Kappa-CCD diffractometers with, for (I)–(IV) and (VI), graphite-monochromated Mo $K\alpha$ radiation (λ = 0.71073 Å) and, for (V), synchrotron radiation (λ = 0.69000 Å). Other details of cell data, data collection and refinement are summarized in Table 1, together with details of the software employed (Farrugia, 1999; Ferguson, 1999; Nonius, 1997; Otwinowski & Minor, 1997; Sheldrick, 1997; Spek, 2003). For (I)–(V) the systematic absences permitted $P2_1$ and $P2_1/m$ as possible space groups: in each case $P2_1$ was selected and confirmed by the structure analysis. Crystals of (VI) are triclinic and the space group $P\overline{1}$ was selected, and confirmed by the structure analysis. The structures were solved by direct methods and refined with all data on F^2. A weighting scheme based upon $P = [F_o^2 + 2F_2]/3$ was employed in order to reduce statistical bias (Wilson, 1976). All H atoms were located from difference maps and all were fully ordered. All H atoms were treated as riding atoms with distances C—H 0.95 (aromatic), 0.98 (methyl) or 1.00 (aliphatic CH), N—H 0.91 and O—H 0.84 Å.

Supramolecular analyses were made and the diagrams were prepared with the aid of *PLATON* (Spek, 2003). Details of hydrogen-bond dimensions are given in Table 2.[1] Figs. 1–16 show the ionic components, with the atom-labelling schemes, and aspects of the supramolecular structures.

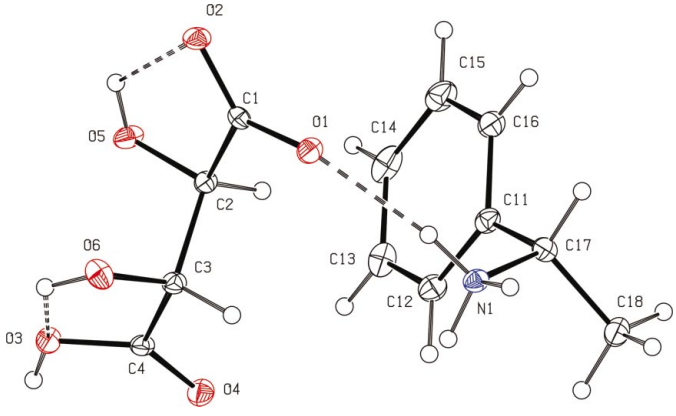

Figure 1
The independent components of (I) showing the atom-labelling scheme. Displacement ellipsoids are drawn at the 30% probability level.

3. Results and discussion

3.1. Crystallization characteristics

Crystallization from methanol solutions of equimolar mixtures of 1-phenylethylamine and tartaric acid gives, regardless of whether the compounds are enantiopure or racemic mixtures, salts of the composition $[PhCH(CH_3)NH_3]^+\cdot[HOCOCH(OH)CH(OH)COO]^-$, in

[1] Supplementary data for this paper are available from the IUCr electronic archives (Reference: BM5020). Services for accessing these data are described at the back of the journal.

Table 1
Experimental details.

	(I)	(II)	(III)
Crystal data			
Chemical formula	$C_8H_{12}N{\cdot}C_4H_5O6$	$C_8H_{12}N{\cdot}C_4H_5O_6$	$C_8H_{12}N{\cdot}C_4H_5O_6$
M_r	271.27	271.27	271.27
Cell setting, space group	Monoclinic, $P2_1$	Monoclinic, $P2_1$	Monoclinic, $P2_1$
a, b, c (Å)	6.3425 (2), 13.9448 (3), 7.5021 (3)	7.3025 (2), 22.8901 (11), 8.1193 (3)	7.2952 (2), 22.8935 (11), 8.1100 (3)
α, β, γ (°)	107.6599 (14)	96.599 (2)	96.603 (2)
V (Å^3)	632.25 (4)	1348.19 (9)	1345.49 (9)
Z, Z'	2, 1	4, 2	4, 2
D_x (Mg m^{-3})	1.425	1.336	1.339
Radiation type	Mo $K\alpha$	Mo $K\alpha$	Mo $K\alpha$
No. of reflections for cell parameters	1497	3191	9403
θ range (°)	2.9–27.5	2.7–27.7	2.7–27.5
μ (mm^{-1})	0.12	0.11	0.11
Temperature (K)	150 (1)	150 (1)	150 (1)
Crystal form, colour	Block, colourless	Needle, colourless	Block, colourless
Crystal size (mm)	0.30 × 0.25 × 0.22	0.28 × 0.16 × 0.14	0.36 × 0.26 × 0.20
Data collection			
Diffractometer	Kappa-CCD	Kappa-CCD	Kappa-CCD
Data collection method	φ scans, and ω scans with κ offsets	φ scans, and ω scans with κ offsets	φ scans, and ω scans with κ offsets
Absorption correction	Multi-scan	Multi-scan	Multi-scan
T_{min}	0.923	0.584	0.869
T_{max}	0.983	0.998	0.991
No. of measured, independent and observed reflections	5067, 1497, 1386	15 852, 3191, 2734	9403, 3160, 2446
Criterion for observed reflections	$I > 2\sigma(I)$	$I > 2\sigma(I)$	$I > 2\sigma(I)$
R_{int}	0.042	0.129	0.061
θ_{max} (°)	27.5	27.7	27.5
Range of h, k, l	$-8 \Rightarrow h \Rightarrow 7$ $-17 \Rightarrow k \Rightarrow 18$ $-9 \Rightarrow l \Rightarrow 9$	$-9 \Rightarrow h \Rightarrow 9$ $-29 \Rightarrow k \Rightarrow 29$ $-8 \Rightarrow l \Rightarrow 10$	$-9 \Rightarrow h \Rightarrow 9$ $-27 \Rightarrow k \Rightarrow 29$ $-9 \Rightarrow l \Rightarrow 10$
Refinement			
Refinement on	F^2	F^2	F^2
$R[F^2 > 2\sigma(F^2)]$, $wR(F^2)$, S	0.032, 0.077, 1.09	0.047, 0.130, 1.06	0.040, 0.091, 1.04
No. of reflections	1497	3191	3160
No. of parameters	177	354	354
H-atom treatment	Constrained to parent site	Constrained to parent site	Constrained to parent site
Weighting scheme	$w = 1/[\sigma^2(F_o^2) + (0.0419P)^2 + 0.0759P]$, where $P = (F_o^2 + 2F_c^2)/3$	$w = 1/[\sigma^2(F_o^2) + (0.0713P)^2 + 0.0775P]$, where $P = (F_o^2 + 2F_c^2)/3$	$w = 1/[\sigma^2(F_o^2) + (0.0449P)^2 + 0.0771P]$, where $P = (F_o^2 + 2F_c^2)/3$
$(\Delta/\sigma)_{max}$	<0.0001	<0.0001	0.001
$\Delta\rho_{max}$, $\Delta\rho_{min}$ (e Å^{-3})	0.16, −0.20	0.34, −0.24	0.18, −0.21
Extinction method	None	*SHELXL*	*SHELXL*
Extinction coefficient	–	0.039 (6)	0.020 (3)

	(IV)	(V)	(VI)
Crystal data			
Chemical formula	$2C_8H_{12}N{\cdot}C_4H_4O_6$	$2C_8H_{12}N{\cdot}C_4H_4O_6$	$4C_8H_{12}N{\cdot}2C_4H_4O_6{\cdot}CH_4O$
M_r	392.44	392.44	816.93
Cell setting, space group	Monoclinic, $P2_1$	Monoclinic, $P2_1$	Triclinic, $P1$
a, b, c (Å)	5.5620 (2), 16.0630 (3), 11.8260 (4)	8.3381 (14), 22.738 (4), 10.8190 (18)	9.0822 (3), 15.7819 (5), 15.9040 (5)
α, β, γ (°)	90.00, 103.2810 (12), 90.00	90.00, 90.120 (3), 90.00	108.7460 (15), 96.858 (2), 90.0600 (18)
V (Å3)	1028.31 (5)	2051.2 (6)	2141.33 (12)
Z, Z'	2, 1	4, 2	2, 2
D_x (Mg m^{-3})	1.267	1.271	1.267
Radiation type	Mo $K\alpha$	Synchrotron	Mo $K\alpha$
No. of reflections for cell parameters	2434	5818	9771
θ range (°)	3.1–27.5	1.7–29.4	2.6–27.6
μ (mm^{-1})	0.09	0.09	0.09
Temperature (K)	150 (1)	150 (1)	150 (1)
Crystal form, colour	Plate, colourless	Plate, colourless	Plate, colourless
Crystal size (mm)	0.36 × 0.26 × 0.10	0.30 × 0.22 × 0.06	0.20 × 0.16 × 0.08
Data collection			
Diffractometer	Kappa-CCD	Kappa-CCD	Kappa-CCD
Data collection method	φ scans, and ω scans with κ offsets	φ scans, and ω scans with κ offsets	φ scans, and ω scans with κ offsets
Absorption correction	Multi-scan	Multi-scan	Multi-scan
T_{min}	0.877	0.972	0.975

Table 1 (continued)

	(IV)	(V)	(VI)
T_{max}	0.995	0.994	0.993
No. of measured, independent and observed reflections	8194, 2434, 2187	18 641, 5818, 5504	28 530, 9771, 6899
Criterion for observed reflections	$I > 2\sigma(I)$	$I > 2\sigma(I)$	$I > 2\sigma(I)$
R_{int}	0.050	0.034	0.094
θ_{max} (°)	27.5	29.4	27.6
Range of h, k, l	$-7 \Rightarrow h \Rightarrow 7$ $-20 \Rightarrow k \Rightarrow 19$ $-14 \Rightarrow l \Rightarrow 15$	$-11 \Rightarrow h \Rightarrow 11$ $-30 \Rightarrow k \Rightarrow 30$ $-15 \Rightarrow l \Rightarrow 14$	$-11 \Rightarrow h \Rightarrow 11$ $-20 \Rightarrow k \Rightarrow 17$ $-19 \Rightarrow l \Rightarrow 20$
Refinement			
Refinement on	F^2	F^2	F^2
$R[F^2 > 2\sigma(F^2)]$, $wR(F^2)$, S	0.035, 0.094, 1.05	0.054, 0.151, 1.16	0.051, 0.132, 1.04
No. of reflections	2434	5818	9771
No. of parameters	260	517	1074
H-atom treatment	Constrained to parent site	Constrained to parent site	Constrained to parent site
Weighting scheme	$w = 1/[\sigma^2(F_o^2) + (0.0574P)^2 + 0.0872P]$, where $P = (F_o^2 + 2F_c^2)/3$	$w = 1/[\sigma^2(F_o^2) + (0.0842P)^2 + 0.5384P]$, where $P = (F_o^2 + 2F_c^2)/3$	$w = 1/[\sigma^2(F_o^2) + (0.066P)^2]$, where $P = (F_o^2 + 2F_c^2)/3$
$(\Delta/\sigma)_{max}$	<0.0001	0.001	0.001
$\Delta\rho_{max}$, $\Delta\rho_{min}$ (e Å^{-3})	0.22, −0.24	0.59, −0.33	0.44, −0.40
Extinction method	*SHELXL*	None	*SHELXL*
Extinction coefficient	0.036 (7)	–	0.0191 (18)

Computer programs used: *Kappa-CCD server software* (Nonius, 1997), *DENZO-SMN* (Otwinowski & Minor, 1997), *SHELXS*97 (Sheldrick, 1997), *SHELXL*97 (Sheldrick, 1997), *PLATON* (Spek, 2003), *PRPKAPPA* (Ferguson, 1999).

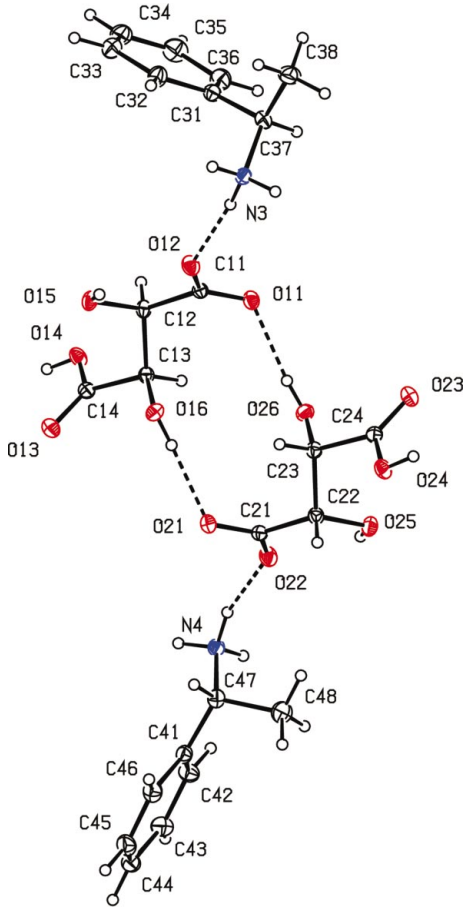

Figure 2
The independent components of (III) showing the atom-labelling scheme. Displacement ellipsoids are drawn at the 30% probability level.

which complete transfer of a single H atom from the acid component to the basic components has occurred.

When enantiopure (S)-amine was cocrystallized with enantiopure (*R*,*R*)-acid, the salt (I) was produced in which the asymmetric unit (Fig. 1) consists of just one cation and one anion. The identical salt was identified as the sole crystalline product from the cocrystallization of the racemic amine and the enantiopure (*R*,*R*)-acid, so that complete enantioselectivity in crystallization is apparent with no (*R*) configuration cations present in the crystalline salt. It is of interest to note in this context that no crystalline product of consistent composition could be obtained from cocrystallizations of enantiopure (*R*)-amine with enantiopure (*R*,*R*)-acid: this observation is entirely consistent with the behaviour reported by Molins *et al.* (1989), who were also unable to obtain any crystalline product from this combination of amine and acid.

On the other hand, when the enantiopure (*S*)-amine was cocrystallized with racemic tartaric acid, the product (II) was found to have an asymmetric unit containing two cations, both of (*S*) configuration, and two anions, one each of (*R*,*R*) and (*S*,*S*) configuration. The enantiomorphous compound (III) was obtained from enantiopure (*R*)-amine and the racemic acid. Hence, although the enantiopure acid exerts selectivity on the racemic amine in the formation of (I), the enantiopure amine has not exerted any selectivity in the formation of (II) and (III). The refinement for (III) is rather better than that for (II) and hence we discuss only (III) (Fig. 2) hereafter.

When the initial crystallization mixtures contained a 2:1 molar ratio of amine to acid, the resulting salts all had the composition $[\{PhCH(CH_3)NH_3\}^+]_2{\cdot}[OOCCH(OH)CH(OH)COO]^{2-}$, again regardless of whether enantiopure or racemic components were employed. Cocrystallization of such a 2:1

Table 2
Hydrogen-bond parameters (Å, °).

	D—H···A	H···A	D···A	D—H···A
(A) Intra-anion hydrogen bonds				
(I)	O5—H5···O2	2.11	2.616 (2)	119
	O6—H6···O3	2.17	2.652 (2)	116
(III)	O15—H15···O12	2.13	2.605 (2)	116
	O25—H25···O22	2.11	2.604 (2)	117
(IV)	O5—H5···O6	2.46	2.860 (2)	110
	O6—H6···O3	2.11	2.603 (2)	117
(V)	None			
(VI)	O15—H15···O12	2.37	2.661 (4)	101
	O25—H25···O22	2.38	2.675 (4)	101
	O45—H45···O42	2.38	2.677 (4)	101
(B) Inter-anion hydrogen bonds				
(I)	O3—H3···O1^{i}	1.65	2.486 (2)	174
	O5—H5···O4^{ii}	2.18	2.797 (2)	130
(III)	O14—H14···O11^{iii}	1.73	2.568 (2)	176
	O15—H15···O22^{iv}	2.22	2.944 (3)	144
	O16—H16···O21	1.92	2.750 (3)	170
	O24—H24···O21^{ii}	1.74	2.575 (2)	177
	O25—H25···O12^{i}	2.35	3.019 (3)	136
	O26—H26···O11	1.94	2.773 (3)	169
(IV)	O5—H5···O1^{iii}	2.07	2.882 (2)	161
(V)	O15—H15···O22^{iii}	1.91	2.743 (3)	169
	O16—H16···O23^{iv}	1.87	2.690 (3)	164
	O25—H25···O11	1.86	2.681 (3)	167
	O26—H26···O13^{v}	1.91	2.743 (3)	169
(VI)	O16—H16···O21	1.90	2.722 (4)	167
	O26—H26···O11	1.89	2.712 (4)	168
	O36—H36···O41	1.91	2.741 (4)	171
	O46—H46···O31	1.88	2.711 (4)	171
	O15—H15···O34^{ii}	1.84	2.628 (4)	156
	O25—H25···O44^{vi}	1.82	2.584 (4)	150
	O35—H35···O14	1.83	2.617 (4)	156
	O45—H45···O24^{vii}	1.82	2.585 (4)	150
(C) Cation–anion hydrogen bonds				
(I)	N1—H1A···O1	2.00	2.901 (2)	172
	N1—H1B···O5^{viii}	2.02	2.867 (2)	154
	N1—H1C···O2^{iii}	1.93	2.842 (2)	177
(III)	N3—H3A···O26^{iv}	2.11	2.945 (3)	152
	N3—H3A···O23^{iv}	2.35	2.893 (3)	118
	N3—H3B···O15^{ii}	1.96	2.847 (3)	165
	N3—H3C···O12	1.85	2.747 (3)	167
	N4—H4A···O16^{i}	2.15	2.956 (3)	147
	N4—H4A···O13^{i}	2.25	2.916 (3)	129
	N4—H4B···O25^{iii}	1.93	2.824 (3)	169
	N4—H4C···O22	1.87	2.752 (3)	162
(IV)	N1—H1A···O2^{ix}	1.88	2.759 (2)	161
	N1—H1B···O4	1.93	2.823 (2)	167
	N1—H1C···O1^{x}	1.89	2.745 (2)	155
	N2—H2A···O2	1.84	2.746 (2)	172
	N2—H2B···O2^{x}	1.91	2.774 (2)	158
	N2—H2C···O3^{ii}	1.85	2.720 (2)	159
(V)	N3—H3A···O12	1.90	2.801 (3)	171
	N3—H3B···O22	1.82	2.718 (4)	168
	N3—H3C···O14^{ii}	1.89	2.777 (3)	165
	N4—H4A···O23^{viii}	1.85	2.738 (3)	165
	N4—H4B···O12^{iii}	1.92	2.825 (3)	170
	N4—H4C···O14	1.98	2.798 (3)	149
	N5—H5A···O21^{viii}	1.89	2.774 (3)	164
	N5—H5B···O24^{iv}	1.89	2.798 (3)	173
	N5—H5C···O13	1.83	2.716 (3)	164
	N6—H6A···O24	1.95	2.847 (3)	171
	N6—H6B···O21^{iii}	1.96	2.803 (3)	154
	N6—H6C···O11	1.86	2.747 (3)	164
(VI)	N5—H5A···O23^{vii}	1.98	2.885 (4)	171
	N5—H5B···O22^{xi}	1.99	2.882 (4)	168
	N5—H5C···O46	2.00	2.902 (4)	173
	N6—H6A···O45	2.10	2.973 (4)	161
	N6—H6B···O22^{xi}	1.96	2.858 (4)	169
	N6—H6C···O11^{vii}	1.89	2.768 (4)	160
	N7—H7A···O43^{iii}	2.01	2.898 (4)	167
	N7—H7B···O42	1.95	2.859 (4)	173
	N7—H7C···O26^{vii}	2.00	2.906 (4)	178
	N8—H8A···O33^{ii}	1.93	2.822 (4)	168
	N8—H8B···O16	2.03	2.912 (4)	163
	N8—H8C···O32	1.96	2.869 (4)	175
	N9—H9A···O41^{ii}	1.93	2.832 (4)	169
	N9—H9B···O32	2.00	2.891 (4)	167
	N9—H9C···O15	1.92	2.825 (4)	174
	N10—H10A···O36	2.04	2.920 (4)	162
	N10—H10B···O12^{iii}	1.95	2.852 (4)	173
	N10—H10C···O13	1.93	2.819 (4)	165
	N11—H11A···O42^{xii}	1.96	2.863 (4)	171
	N11—H11B···O31^{vi}	1.91	2.781 (4)	160
	N11—H11C···O25	2.03	2.918 (4)	163
	N12—H12A···O21	1.93	2.832 (4)	170
	N12—H12B···O12^{iii}	2.00	2.906 (4)	172
	N12—H12C···O35	1.94	2.844 (4)	177
(D) Cation–cation hydrogen bonds				
(III)	C36—H36···Cg^{ix}†	2.87	3.775 (3)	160
(E) Solvent–anion hydrogen bonds				
(VI)	O1—H1···O23	1.90	2.730 (5)	170
	O2—H2···O43	1.97	2.791 (5)	164

Symmetry codes: (i) $x, y, -1+z$; (ii) $-1+x, y, z$; (iii) $1+x, y, z$; (iv) $x, y, 1+z$; (v) $-1+x, y, -1+z$; (vi) $x, -1+y, z$; (vii) $1+x, 1+y, z$; (viii) $1+x, y, 1+z$; (ix) $1-x, -\frac{1}{2}+y, 1-z$; (x) $-x, -\frac{1}{2}+y, 1-z$; (xi) $x, 1+y, z$; (xii) $-1+x, -1+y, z$. † Cg represents the ring centroid of the ring C41–C46.

mixture containing enantiopure (*S*)-amine and enantiopure (*R*,*R*)-acid yielded a product (IV) containing two cations and one anion in the asymmetric unit (Fig. 3). In contrast to the behaviour of the 1:1 mixture producing (I), a 2:1 mixture of racemic amine and enantiopure (*R*,*R*)-acid gave a product (V) in which the asymmetric unit (Fig. 4) consists of four cations, two each of (*R*) and (*S*) configurations, and two anions, so that no enantioselectivity is apparent here.

Each of the salts (I)–(V) crystallizes in the space group $P2_1$. However, the salt (VI) produced from a 2:1 mixture of enantiopure (*R*)-amine and racemic tartaric acid crystallizes in

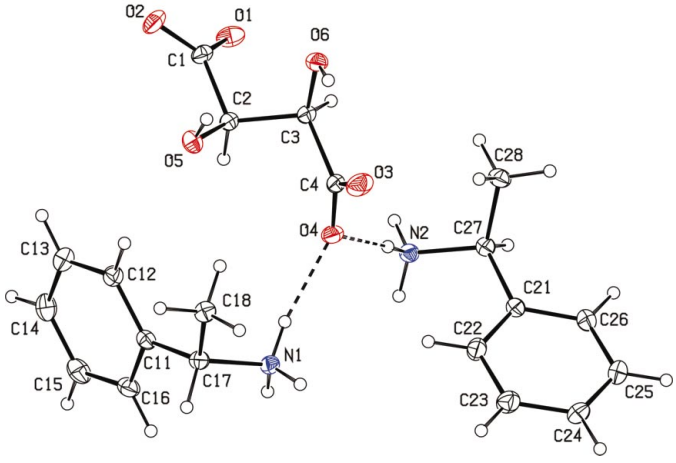

Figure 3
The independent components of (IV) showing the atom-labelling scheme. Displacement ellipsoids are drawn at the 30% probability level.

the space group *P*1 and its asymmetric unit (Fig. 5) contains eight cations and four anions, of which two each have (*R*,*R*) and (*S*,*S*) configurations, together with two methanol molecules. A product (VII) of identical composition was isolated from a 2:1 mixture of the enantiopure (*S*)-amine and racemic tartaric acid, but no crystals suitable for single-crystal X-ray diffraction have yet been obtained.

3.2. Structure solutions

Although in each of (I)–(VI) the Flack parameter (Flack, 1983) was wholly inconclusive (Flack & Bernardinelli, 2000) because of the very low anomalous dispersion characteristic of the light elements C, N and O, nonetheless, in every case the initial structure solution, obtained using *System-S* in *PLATON* (Spek, 2003), corresponded to the correct enantiomorph of the enantiopure component present.

Struck by this rather unexpected result, we have now reviewed our initial structure solutions for some recently completed series of light-atom structures containing enantiopure components of previously known configuration, namely series containing malate and tartrate anions (Farrell *et al.*, 2002*a*,*b*; Bowes *et al.*, 2003*b*; Turkington *et al.*, 2004). In a total of 17 structures, including those reported here, each having a chiral space group containing an enantiopure component of previously known configuration, the initial structure solution using *System-S* gave the correct enantiomorph in every case, without exception.

3.3. Intra-anion hydrogen bonds

The intra-anion hydrogen bonding (Table 2), in principle the simplest aspect of the hydrogen bonding, nonetheless shows several variants, several of which are not readily predictable. In the independent anion of (III), and in three of the four independent anions in (VI), there is a single intra-anion hydrogen bond and in every case the acceptor is a carboxylate O atom. In the fourth anion in (VI), no such bond occurs nor is there any such bond in either of the anions in (V). In (I) and (IV), on the other hand, both hydroxyl groups in the anion form intra-anion hydrogen bonds; in (I) both acceptors are carboxyl O atoms, while for (III) the acceptor in one interaction is a carboxylate O, as usual, while in the other it is the second hydroxyl O. For none of these hydrogen bonds does the O—H···O angle exceed 120°, so that the interaction energies may well be fairly small: however, the entropic cost of these interactions is almost negligible and they may well have a significant influence on the overall anion conformations.

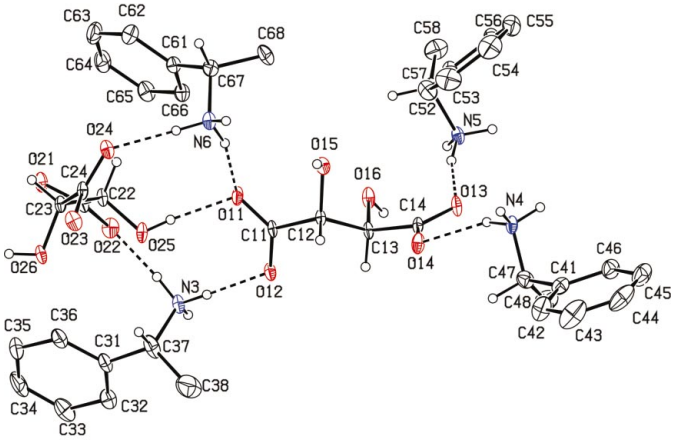

Figure 4
The independent components of (V) showing the atom-labelling scheme. Displacement ellipsoids are drawn at the 30% probability level.

3.4. Anion substructures

In the supramolecular structures of each of (I)–(VI) there is a clearly identifiable substructure built from only the anions. It is convenient to approach the overall analysis of the supramolecular structures firstly in terms of these anion substructures and then to consider how the cations, and in (VI) only the methanol molecules, are linked to the anion substructure.

3.4.1. Compound (I). The anions in (I) form a two-dimensional substructure which is generated wholly by translation. Carboxyl O3 in the anion at (x, y, z) acts as a donor to carboxylate O1 in the anion at $(x, y, -1 + z)$ in a very short hydrogen bond, so generating a $C(7)$ (Bernstein *et al.*, 1995) chain running parallel to the [001] direction. The hydroxyl O5, as well as acting as a hydrogen-bond donor to O2 within the anion, also acts as a donor to carbonyl O4 in the anion at $(-1 + x, y, z)$, in a planar three-centre O—H···$(O)_2$ system, so generating a $C(6)$ chain parallel to [100]. The combination of the [100] and [001] chains generates a (010) sheet in the form of a (4,4) net (Batten & Robson, 1998) built from a single type of $R_4^4(22)$ ring (Fig. 6). The reference anion sheet lies in the domain $0.27 < y < 0.47$ and a second such sheet, related to the first by the action of the 2_1 screw axis, lies in the domain $0.77 < y < 0.97$.

3.4.2. Compound (III). The two independent anions in (III) form a two-dimensional substructure which is generated wholly by translation. Within the asymmetric unit (Fig. 2), hydroxyl atoms O16 and O26 act as hydrogen-bond donors, respectively, to carboxylate atoms O21 and O11, and these $R_2^2(12)$ dimers are linked by two further pairs of O—H···O hydrogen bonds into chains of edge-fused rings running along the [100] and [001] directions. Carboxyl atoms O14 and O24 in the anion pair at (x, y, z) act as donors, respectively, to carboxylate atoms O11 at $(1 + x, y, z)$ and O21 at $(-1 + x, y, z)$, thereby generating by translation a chain of edge-fused, alternating $R_2^2(12)$ and $R_2^4(14)$ rings, in which the carboxylate atoms O11 and O21 both act as double acceptors of O—H···O hydrogen bonds. In addition, the two hydroxyl atoms O15 and O25 at (x, y, z) act as donors, respectively, to carboxylate atoms O22 at $(x, y, 1 + z)$ and O12 at $(x, y, -1 + z)$, thereby generating by translation a second chain of edge-fused rings, this time running parallel to the [001] direction and containing alternating $R_2^2(12)$ and $R_2^2(10)$ rings. The combination of the [100] and [001] chains generates a (010) sheet built from four different types of ring, $R_2^2(10)$, $R_2^2(12)$, $R_2^4(14)$ and $R_4^4(20)$ (Fig. 7). The first two ring types each involve one (2*R*,3*R*) anion and one (2*S*,3*S*) anion, while the latter two types involve two anions of each hand; each ring is

therefore approximately, but not crystallographically, centrosymmetric. The hydrogen-bonded anion sheet is modestly reinforced by an antiparallel and nearly centrosymmetric carbonyl–carbonyl interaction involving the groups C14═O13 and C24═O23 in the anions at (x, y, z) and $(1 + x, y, z)$, respectively. The distances O13···C14^{i} and C14···O23^{i} [symmetry code (i) $1 + x, y, z$] are 2.887 (3) and 2.865 (3) Å, respectively, with angles C14—O13···C24^{i} and C14···O23^{i}—C24^{i} of 92.9 (2) and 94.2 (2)°, respectively, hence forming an almost ideal type-II interaction (Allen *et al.*, 1998). The reference anion sheet lies in the domain $0.38 < y < 0.59$, with the $R_2^2(12)$ anion dimers all centred at around $y = 0.50$; the immediately adjacent sheets, related to the first by the action of the 2_1 screw axis, lie in the domain $-0.12 < y < 0.09$ and $0.88 < y < 1.09$, with their $R_2^2(12)$ anion dimers centred at around $y = 0.0$ and $y = 1.0$, respectively.

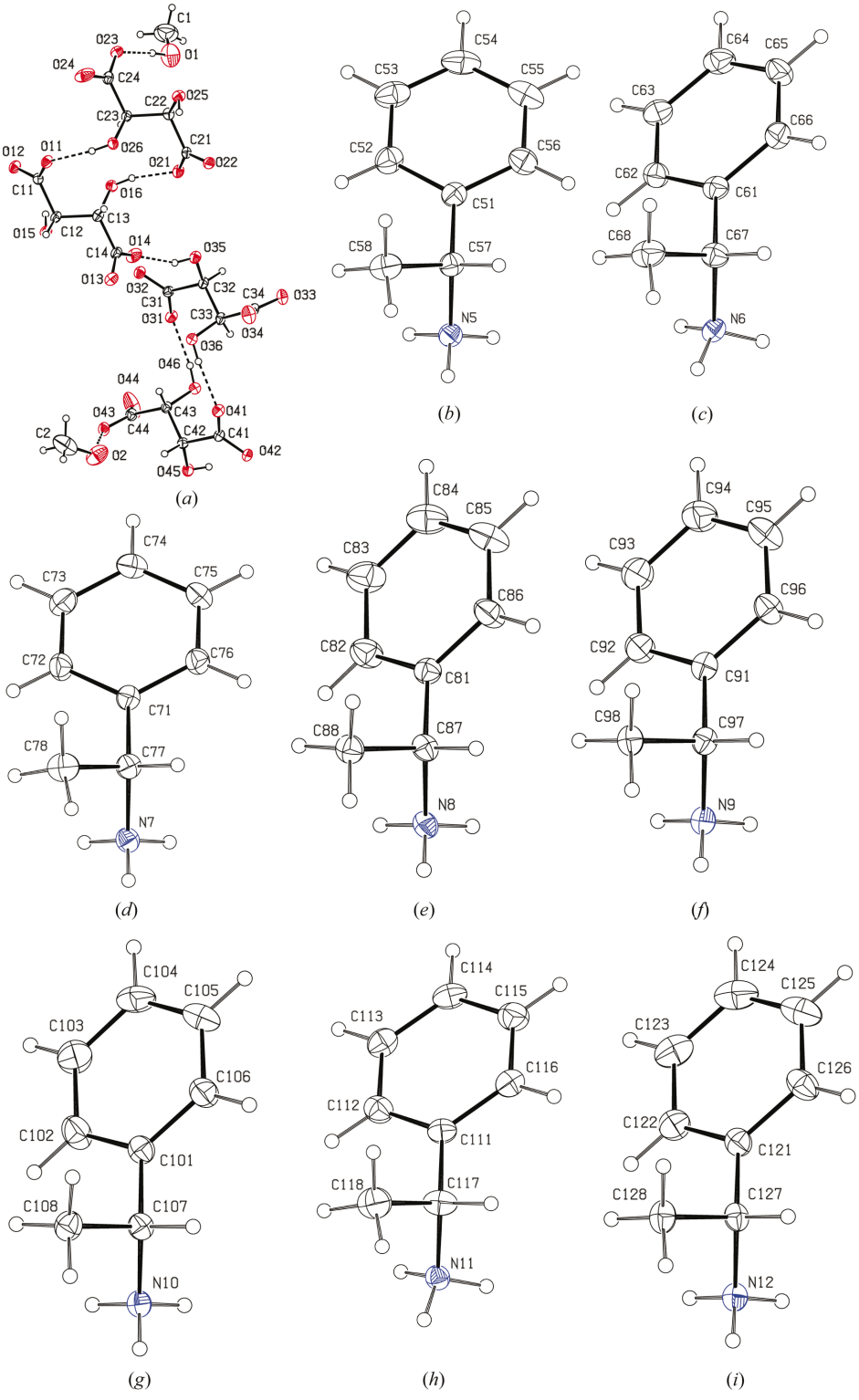

Figure 5
The independent components of (VI) showing the atom-labelling scheme: (*a*) the four independent anions and the two methanol molecules; (*b*)–(*i*) the eight independent cations. Displacement ellipsoids are drawn at the 30% probability level.

3.4.3. Compound (IV). The anion substructure of (IV) consists of simple chains generated by translation. The hydroxyl atom O5 in the anion at (x, y, z) acts as a hydrogen-bond donor to the carboxylate atom O1 in the anion at $(1 + x, y, z)$, so generating by translation a $C(5)$ chain running parallel to the [100] direction (Fig. 8). This chain lies in the domain $0.54 < y < 0.85$, and a second chain, related to the first by the action of the 2_1 screw axis, lies in the domain $0.04 < y < 0.35$: the [100] chains are linked into sheets by the two types of cation.

3.4.4. Compound (V). In (V) there are two independent tartrate anions, albeit both with the (*R*,*R*) configuration, and there are four independent O—H···O hydrogen bonds which link the anions into sheets generated by translation. With the asymmetric unit (Fig. 4), the hydroxyl atom O25 acts as a hydrogen-bond donor to the carboxylate atom O11. The hydroxyl atom O15 in the anion pair at (x, y, z) acts as a donor to the carboxylate atom O22 in the anion pair at $(1 + x, y, z)$, thus generating by translation a $C_2^2(10)$ chain running parallel to the [100] direction. Similarly, the hydroxyl atom O16 at (x, y, z) acts as a donor to the carboxylate atom O23 at $(x, y, 1 + z)$, so generating a second chain by translation, this time of $C22(12)$ type and running parallel to

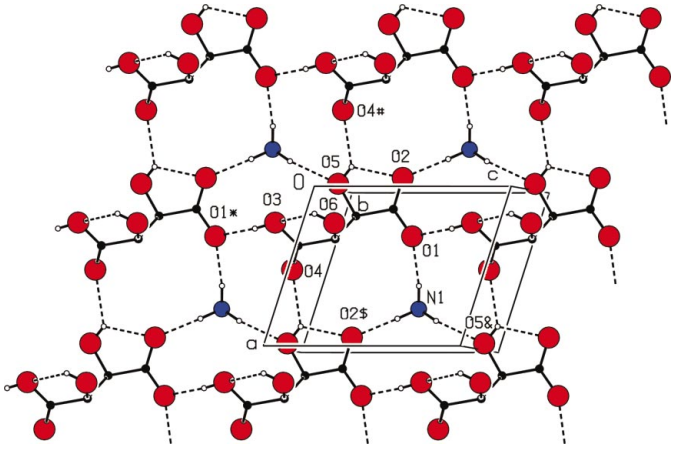

Figure 6
Part of the crystal structure of (I) showing the formation of a (010) sheet of anions with cations pendent from it. For the sake of clarity, the H atoms bonded to the C atoms are omitted, as are the phenyl and methyl groups in the cation. The atoms marked with an asterisk (*), a hash (#), a dollar sign ($) or an ampersand (&) are at the symmetry positions $(x, y, -1+z)$, $(-1+x, y, z)$, $(1+x, y, z)$ and $(1+x, y, 1+z)$, respectively.

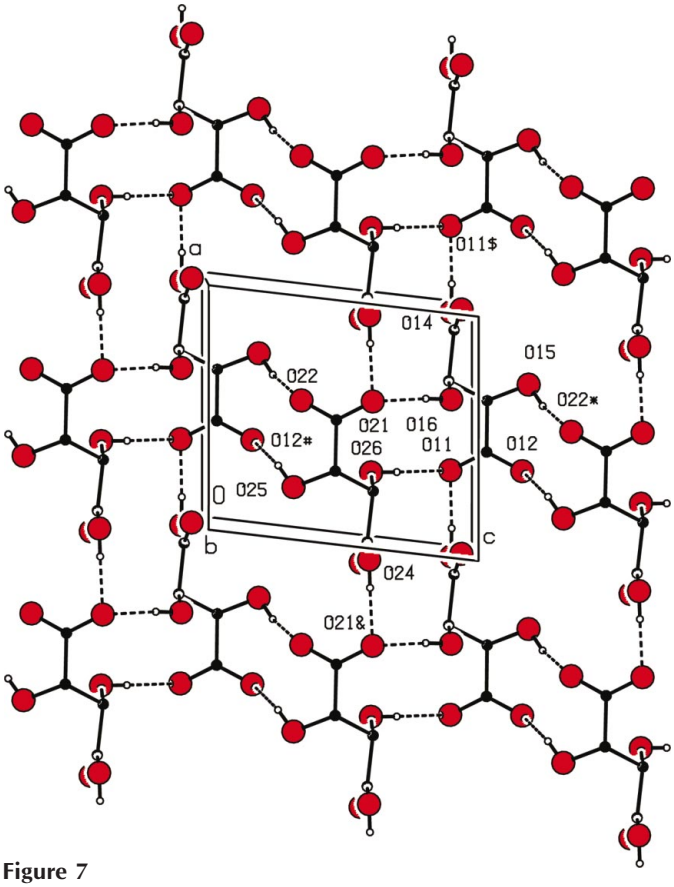

Figure 7
Part of the crystal structure of (III), showing the formation by the anions of a (010) sheet containing four different types of ring. For the sake of clarity, the H atoms bonded to the C atoms are omitted, as are the intra-anion O—H···O hydrogen bonds. The atoms marked with an asterisk (*), a hash (#), a dollar sign ($) or an ampersand (&) are at the symmetry positions $(x, y, 1+z)$, $(x, y, -1+z)$, $(1+x, y, z)$ and $(-1+x, y, z)$, respectively.

the [001] direction. Finally, the hydroxyl atom O26 at (x, y, z) acts as a donor to the carboxylate atom O13 at $(-1+x, y, -1+z)$, thus generating by translation a second $C_2^2(12)$ motif, now running parallel to the [101] direction. The combination of these three translational chain motifs generates a (010) sheet of anions characterized by two different types of $R_4^4(22)$ ring (Fig. 9).

This reference sheet of anions lies within the domain $0.42 < y < 0.59$ and a second such sheet, related to the first by the action of the 2_1 screw axes, lies in the domain $-0.08 < y < 0.09$. The large spaces between the nearly planar anion layers are occupied by the cations.

3.4.5. Compound (VI). Despite the presence of 14 independent components in the asymmetric unit of (VI) (Fig. 5), the four independent anions together generate a fairly simple two-dimensional substructure, from which all of the other components, both cations and neutral methanol molecules, are pendent.

Within the anion sheet there are eight independent inter-anion O—H···O hydrogen bonds all involving hydroxyl O as the donor and carboxylate O as the acceptor. Four of these hydrogen bonds link pairs of anions, each comprising one (*R*,*R*) anion and one (*S*,*S*) anion, into two almost centrosymmetric dimers, and the other four O—H···O hydrogen bonds link the dimers into a continuous sheet. Atoms O16 and O26 act as donors, respectively, to atoms O21 and O11, thus generating a nearly centrosymmetric $R_2^2(12)$ dimer, which we denote as the type *A* dimer, whose centroid is close to (0.25,

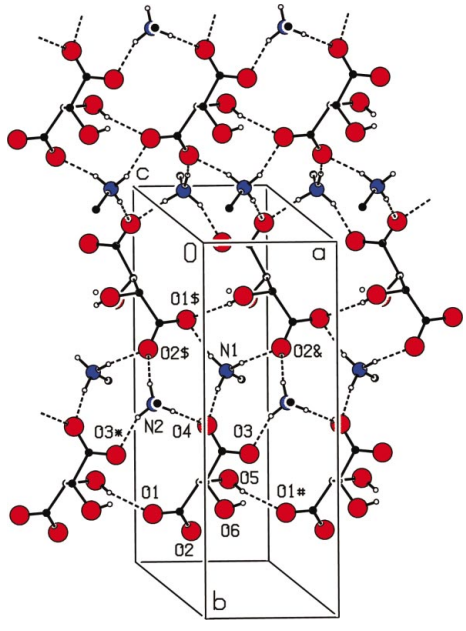

Figure 8
Part of the crystal structure of (IV) showing the formation of the *C*(5) anion chains parallel to [100] and their linking into (001) sheets by the cations. For the sake of clarity, the H atoms bonded to the C atoms are omitted, as are the methyl and phenyl groups in the cations and the intra-anion O—H···O hydrogen bonds. The atoms marked with an asterisk (*), a hash (#), a dollar sign ($) or an ampersand (&) are at the symmetry positions $(-1+x, y, z)$, $(1+x, y, z)$, $(-x, -\frac{1}{2}+y, 1-z)$ and $(1-x, -\frac{1}{2}+y, 1-z)$, respectively.

0.25, 0.5): similarly, atoms O36 and O46 act as donors, respectively, to atoms O41 and O31, thus generating a second nearly centrosymmetric $R_2^2(12)$ dimer, denoted as type *B*, whose centroid is close to (0.75, 0.75, 0.5).

The inter-dimer hydrogen bonds are so arranged that each type *A* dimer acts as a donor to two type *B* dimers and as an acceptor from two further type *B* dimers, while each type *B* dimer is similarly linked to four different type *A* dimers. Thus, for example, in the type *A* dimer at approximately (0.25, 0.25, 0.5), atoms O25 and O15 act as donors, respectively, to the atoms O44 at $(x, -1+y, z)$ and O34 at $(-1+x, y, z)$, which lie in the type *B* dimers at approximately (0.75, −0.25, 0.5) and (−0.25, 0.75, 0.5), respectively: similarly, atoms O14 and O24 in the type *A* dimer at approximately (0.25, 0.25, 0.5) accept hydrogen bonds, respectively, from atoms O35 at (x, y, z) and O45 at $(-1+x, -1+y, z)$, which lie in the type *B* dimers at approximately (0.75, 0.75, 0.5) and (−0.25, −0.25, 0.5), respectively. In this manner, the two types of dimer are linked into a (001) sheet containing two independent $R_2^2(12)$ rings within the dimers and two independent $R_6^6(32)$ rings between the dimers. If the individual anions are taken to be the nodes of the resulting net, this is of the (6,3) type (Batten & Robson, 1998), while if the pseudosymmetric dimers are taken as the nodes the net is of the (4,4) type (Fig. 10). Just one sheet of this type passes through each unit cell, occupying only about one-third of the domain of *z*: for the selected location of the asymmetric unit, the sheet occupies the domain $0.34 < z < 0.68$.

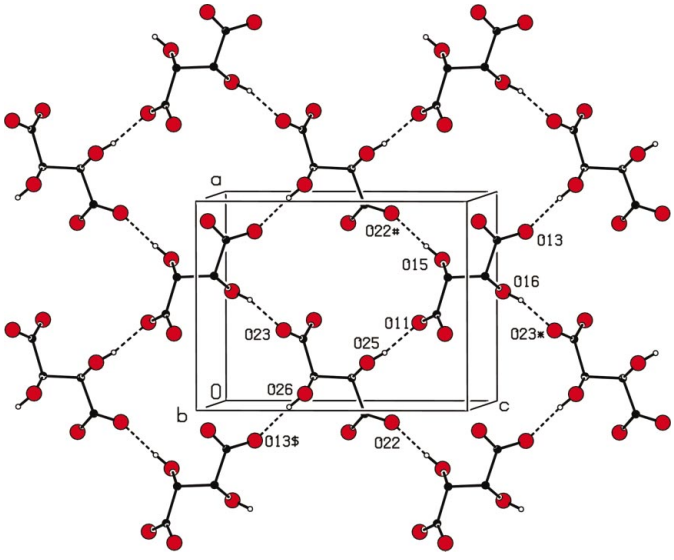

Figure 9
Part of the crystal structure of (V) showing the formation of a (010) anion sheet built from two types of $R_4^4(22)$ ring. For the sake of clarity, the H atoms bonded to C atoms are omitted. The atoms marked with an asterisk (*), a hash (#) or a dollar sign ($) are at the symmetry positions $(x, y, 1+z)$, $(1+x, y, z)$ and $(-1+x, y, -1+z)$, respectively.

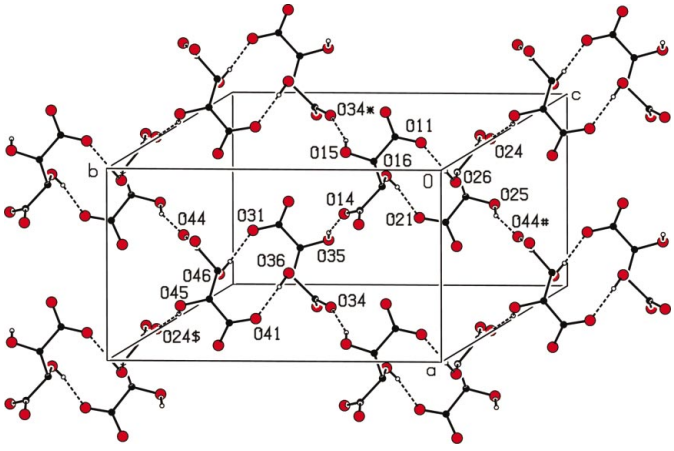

Figure 10
Part of the crystal structure of (VI) showing the formation of a (001) anion sheet built from two types of $R_2^2(12)$ ring and two types of $R_6^6(32)$ ring. For the sake of clarity the H atoms bonded to C atoms are omitted, as are the methyl and phenyl groups in the cations and the intra-anion O—H···O hydrogen bonds. The atoms marked with an asterisk (*), a hash (#) or a dollar sign ($) are at the symmetry positions $(-1+x, y, z)$, $(x, -1+y, z)$ and $(1+x, 1+y, z)$, respectively.

3.5. Linking of the cations to the anion substructures

In each of (I), (III), (V) and (VI) the cations are linked to anion sheets, whereas in (IV) the cations link anion chains into sheets; it is convenient to discuss these two structure types separately. In each of these compounds the $[PhCH(CH_3)NH_3]^+$ cations act as threefold donors in N—H···O hydrogen bonds and each cation is linked to three different anions (Table 2): the majority of these hydrogen bonds are of two-centre type, but three-centre N—H···$(O)_2$ systems occur in (III)

3.5.1. Compounds (I), (III), (V) and (VI). In each of these compounds the three anions which are directly hydrogen-bonded to a given cation form part of the same sheet: however, the orientation of the organic parts of the cations is not the same in each compound. The cations in (I) are all of the (*S*) configuration and all are hydrogen-bonded to just one face of the anion sheet (Fig. 6), so that viewed along the plane of the anion sheet the structure appears to consist of alternating slabs of cations and anions (Fig. 11). In (III), by contrast, there are cations pendent from both faces of the

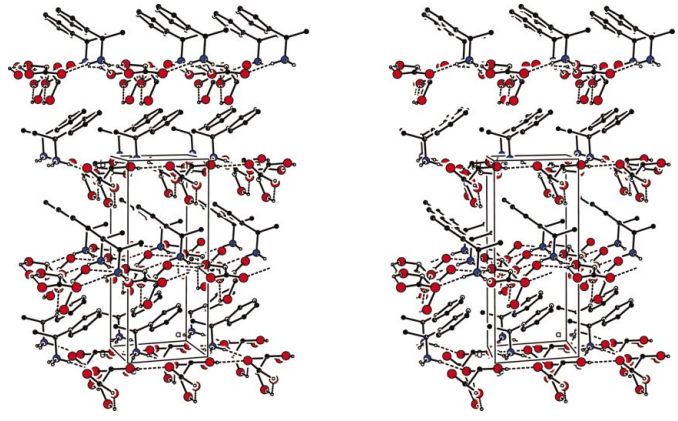

Figure 11
Stereoview of part of the crystal structure of (I) showing the cations pendent from a single face of the anion sheet. For the sake of clarity, the H atoms bonded to the C atoms have been omitted.

anion sheet (Fig. 7), although all have the same (*R*) configuration, with all of the type 1 cations containing N3 pendent from one face and all of the type 2 containing N4 cations pendent from the opposite face. Hence, each (010) layer is tripartite with a polar central layer containing all the hydrogen bonds and two lipophilic outer layers (Fig. 12).

In (V) the cations are again pendent from both faces of the anion sheet (Fig. 9), however, there are cations of both (*R*) and (*S*) configurations bonded to both faces. The cations containing N3 and N4, which have the (*R*) and (*S*) configurations, respectively, are pendent from one face, while the cations containing N5 and N6, again of (*R*) and (*S*) configurations, respectively, are pendent from the opposite face: hence, a tripartite layer is again generated (Fig. 13). All of the cations in (VI) have the (*R*) configuration and four cations are pendent from each face of the sheet: those containing N5, N8, N1 and N12 are pendent from one face, and those containing N6, N7, N9 and N10 are pendent from the other face (Fig. 14).

3.5.2. Compound (IV). The anion substructure in (IV) consists of simple [100] chains generated by translation and the action of the cations is to link these chains into sheets, while the action of the 2_1 screw axes is to cause an alternation of each type of cation, both of (*S*) configuration, between the two faces of these sheets.

The ammonium atom N1 at (x, y, z) acts as a hydrogen-bond donor, *via* H1*B*, to atom O4 in the anion at (x, y, z), which lies in the reference [100] chain, and *via* H1*A* and H1*C* to atoms O2 in the anion at $(1-x, -\frac{1}{2}+y, 1-z)$ and O1 in the anion at $(-x, -\frac{1}{2}+y, 1-z)$, both of which lie in an adjacent [100] chain related to the first chain by the action of the 2_1 screw axes. Atom N2 at (x, y, z) acts as a donor, *via* H2*A* and H2*C*, to atoms O4 in the anion at (x, y, z) and O3 in the anion at $(-1+x, y, z)$, respectively, which both lie in the reference anion chain, and *via* H2*B*, to atom O2 in the anion at $(-x, -\frac{1}{2}+y, 1-z)$, which lie in the adjacent chain referred to previously. In this way the two cations at (x, y, z) are each hydrogen bonded to the same pair of anion chains and propagation of these interactions by the 2_1 screw axes then links the anion chains and the cations into a (001) sheet (Fig. 8). The reference cations containing N1 and N2 have their $PhCH(CH_3)-$ fragments on opposite sides of the sheet, but the action of the screw axes means that there are equal numbers of each of the two cation types on both sides of the sheet (Fig. 15).

3.6. Linking of the sheets in (III)

In none of the compounds described here are there any aromatic $\pi\cdots\pi$ stacking interactions, but in (III) only there is a single C—H$\cdots\pi$(arene) hydrogen bond, whose effect is to link the adjacent tripartite (010) sheets into a continuous framework structure. The aromatic atom C36 in the type 1 cation at (x, y, z), which is pendent from the anion sheet in the domain $0.38 < y < 0.59$, acts as a hydrogen-bond donor to the ring C41–C46 in the type 2 cation at $(1-x, -\frac{1}{2}+y, 1-z)$, which is pendent from the anion sheet in the domain $-0.12 < y < 0.09$, so forming a chain running parallel to the [010] direction and generated by the 2_1 screw axis along $(0.5, y, 0.5)$, which serves to link each (010) sheet to the two adjacent sheets (Fig. 16).

3.7. (*S*)-1-Phenylethylammonium *meso*-hydrogen tartrate

This compound crystallizes in the space group $P2_1$ in a unit cell very similar to that of (I) (Table 1), but with the anion in an almost centrosymmetric configuration (Kroon *et al.*, 1984):

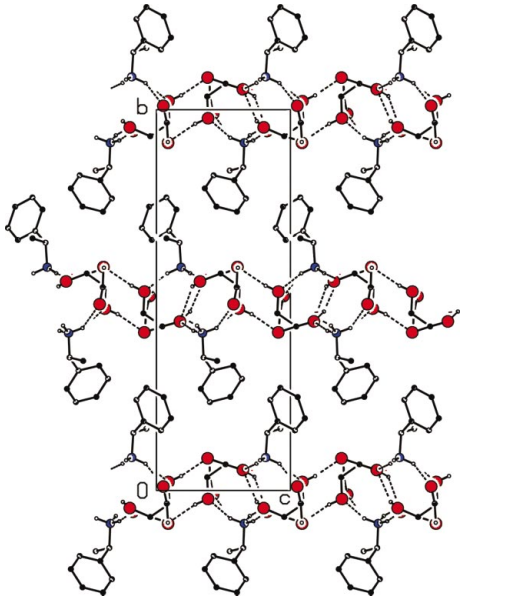

Figure 12
Projection of part of the crystal structure of (III) showing the tripartite (010) layers with cations linked to both faces of the anion sheet. For the sake of clarity, the H atoms bonded to the C atoms have been omitted.

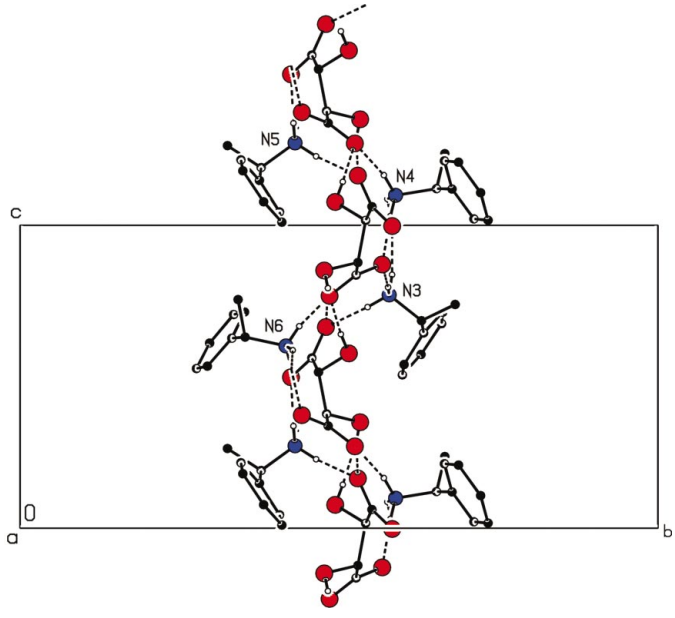

Figure 13
Projection of part of the crystal structure of (V) showing one of the tripartite (010) layers with cations linked to both faces of the anion sheet. For the sake of clarity, the H atoms bonded to C atoms have been omitted.

although no analysis of the supramolecular structure appears in this report, the reported atom coordinates indicate both similarities to, and differences from, that of (I). As in (I), the anions are linked into hydrogen-bonded (010) sheets and the cations are pendent from just one face of this sheet. However, whereas in (I) the sheets contain just a single type of $R_4^4(22)$ ring, in the *meso*-tartrate analogue the sheets contain alternating $R_2^2(10)$ and $R_4^4(20)$ rings.

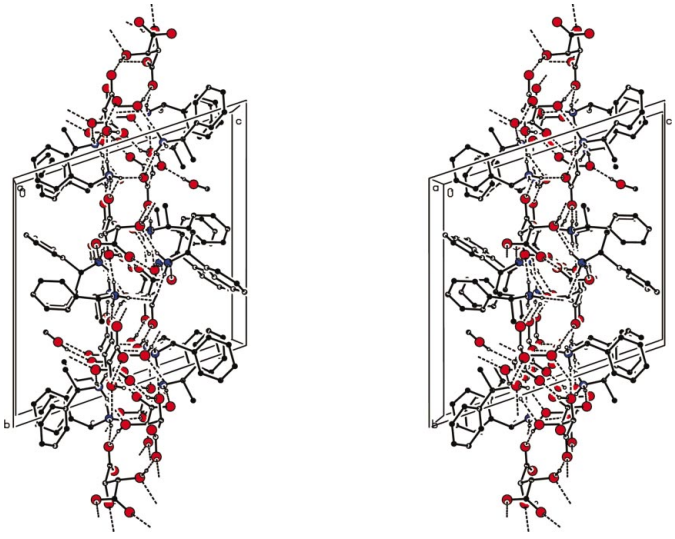

Figure 14
Stereoview of part of the crystal structure of (VI) showing the tripartite sheets and the pendent methanol molecules. For the sake of clarity, the H atoms bonded to C atoms have been omitted.

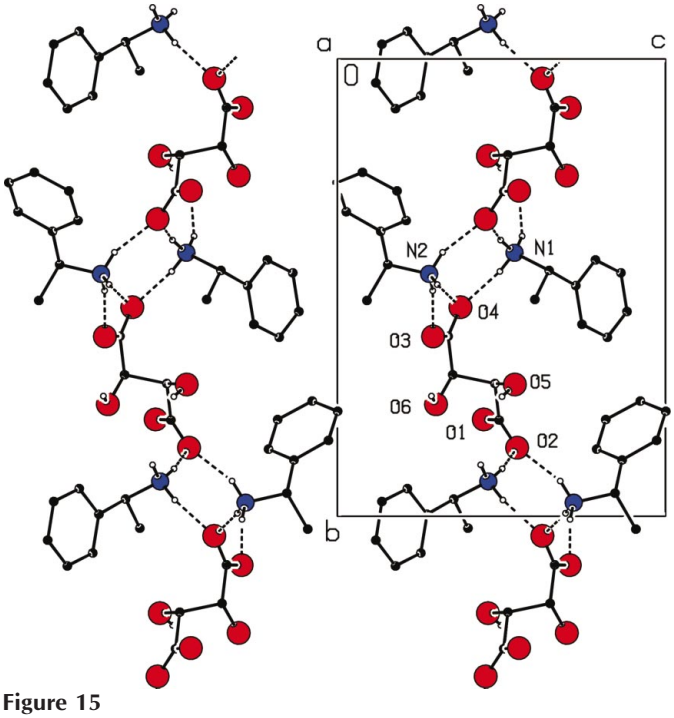

Figure 15
Projection of part of the crystal structure of (IV) showing the cations linked to both faces of the anion sheet, and the action of the 2_1 screw axes in causing alternation of the cations between the two faces. For the sake of clarity, the H atoms bonded to C atoms have been omitted.

3.8. (*R*)-Histidinium (*R*,*R*)-hydrogen tartrate

The supramolecular structure of (*R*)-histidinium (*R*,*R*)-hydrogen tartrate has been reported very recently (Johnson & Feeder, 2004). In this salt, which crystallizes in the space group *P*1 with $Z' = 1$, the anions form (010) sheets of $R_4^4(22)$, formed in a manner entirely similar to those in (I) (see §3.4.1), with one-dimensional substructures in the form of *C*(6) and *C*(7) chains along [100] and [010], respectively, although in (I) the *C*(7) chain is parallel to [001]. The principal difference between the structure of (I) and that of (*R*)-histidinium (*R*,*R*)-hydrogen tartrate arises from the hydrogen-bonding characteristics of the cations. In (I) the cation is a threefold donor in N—H···O hydrogen bonds, whereas in (*R*)-histidinium (*R*,*R*)-hydrogen tartrate the cation is a fivefold donor (although not all of the N—H···O hydrogen bonds are listed in Table 2 of Johnson & Feeder, 2004), and the action of the cation is to link the anion sheets into a continuous three-dimensional framework.

4. Concluding comments

For both the 1:1 salts (I)–(III) and the 2:1 salts (IV)–(VI) described here, modest changes in the stereochemical nature of the components provokes rather considerable changes in the crystallization characteristics, as manifested by a comparison of both the unit-cell dimensions and the Z' values within each series (Table 1). At a more detailed level, no two salts described here, apart from the enantiomorphous pair (II) and (III), have a common anion substructure, and it is notable that we have not observed in any of (I)–(VI) any three-dimen-

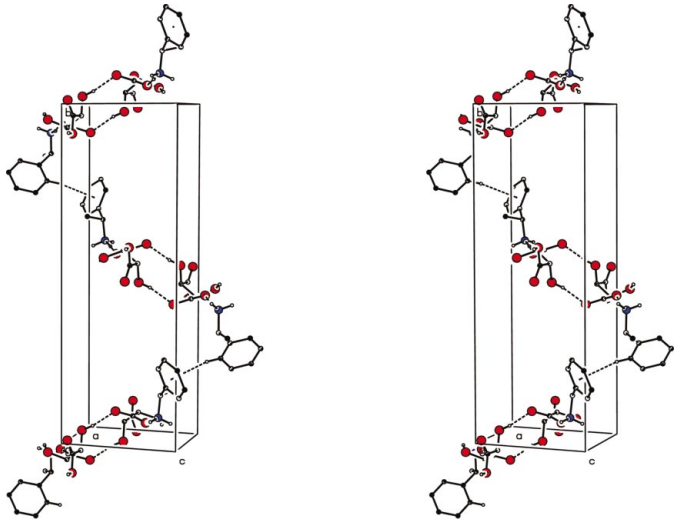

Figure 16
Stereoview of part of the crystal structure of (III) showing the [010] chain built from C—H···π(arene) hydrogen bonds which links the (010) sheets. For the sake of clarity the H atoms not involved in the motif shown have been omitted.

sional anion substructures as observed in the 1:2 salts formed by racemic tartaric acid with each of the simple achiral diamines piperazine and 1,4-diazabicycle[2.2.2]octane (Farrell *et al.*, 2002*a*). In the present series, even when the anion substructures are two-dimensional, the variety and the sizes of the hydrogen-bonded rings from which the sheets are built are different in every case. We have previously observed very marked diversity of supramolecular aggregation in series involving geometrical (constitutional) as opposed to stereochemical (configurational) isomerism (Bowes *et al.*, 2003*a*; Glidewell *et al.*, 2002, 2004). In the salts (I) and (IV), where both components are enantiopure, there is no hint of any mimicry of pseudosymmetry (Figs. 11 and 15). However, in the salts (II), (III) and (VI), where the cations are enantiopure and the anions are racemic, there is strong mimicry of centrosymmetry (Figs. 12 and 14), with weaker indications in (V) (Fig. 9). In general, pseudo-symmetry seems to be manifest in the present series when the anions are racemic, indicating that the formation of the anion sub-structure is a major determinant of the supramolecular structure as a whole.

X-ray data were collected at the University of Toronto using a Nonius Kappa-CCD diffractometer purchased with funds from NSERC Canada. We acknowledge the CCLRC for provision of beamtime on Station 9.8 of the SRS.

References

Allen, F. H., Baalham, C. A., Lommerse, J. P. M. & Raithby, P. R. (1998). *Acta Cryst.* B**54**, 320–329.
Batten, S. R. & Robson, R. (1998). *Angew. Chem. Int. Ed.* **37**, 1460–1494.
Bernstein, J., Davis, R. E., Shimoni, L. & Chang, N.-L. (1995). *Angew. Chem. Int. Ed. Engl.* **34**, 1555–1573.
Bowes, K. F., Ferguson, G., Lough, A. J. & Glidewell, C. (2003*a*). *Acta Cryst.* B**59**, 100–117.
Bowes, K. F., Ferguson, G., Lough, A. J. & Glidewell, C. (2003*b*). *Acta Cryst.* C**59**, o329–o331.
Farrell, D. M. M., Ferguson, G., Lough, A. J. & Glidewell, C. (2002*a*). *Acta Cryst.* B**58**, 272–288.
Farrell, D. M. M., Ferguson, G., Lough, A. J. & Glidewell, C. (2002*b*). *Acta Cryst.* B**58**, 530–544.
Farrugia, L. (1999). *J. Appl. Cryst.* **32**, 837–838.
Ferguson, G. (1999). *PRPKAPPA*. University of Guelph, Canada.
Flack, H. D. (1983). *Acta Cryst.* A**39**, 876–881.
Flack, H. D. & Bernardinelli, G. (2000). *J. Appl. Cryst.* **33**, 1143–1148.
Glidewell, C., Howie, R. A., Low, J. N., Skakle, J. M. S., Wardell, S. M. S. V. & Wardell, J. L. (2002). *Acta Cryst.* B**58**, 864–876.
Glidewell, C., Low, J. N., Skakle, J. M. S., Wardell, S. M. S. V. & Wardell, J. L. (2004). *Acta Cryst.* B**60**, 472–480.
Johnson, M. N. & Feeder, N. (2004). *Acta Cryst.* E**60**, o1476–o1477.
Kroon, J., Duisenberg, A. J. M. & Peerdeman, A. F. (1984). *Acta Cryst.* C**40**, 645–647.
Molins, E., Miravitlles, C., López-Calahorra, F., Castells, J. & Raventós, J. (1989). *Acta Cryst.* C**45**, 104–106.
Nonius (1997). *Kappa-CCD Server Software*, Windows 3.11 Version. Nonius BV, Delft, The Netherlands.
Otwinowski, Z. & Minor, W. (1997). *Methods Enzymol.* **276**, 307–326.
Sheldrick, G. M. (1997). *SHELXS*97 and *SHELXL*97. University of Göttingen, Germany.
Spek, A. L. (2003). *J. Appl. Cryst.* **36**, 7–13.
Turkington, D. E., Ferguson, G., Lough, A. J. & Glidewell, C. (2004). *Acta Cryst.* C**60**, o617–o622.
Wilson, A. J. C. (1976). *Acta Cryst.* A**32**, 994–996.